Quadratic Pulse Inversion Ultrasonic Imaging (QPI): A Two-Step Procedure for Optimization of Contrast Sensitivity and Specificity

Mamoun F. Al-Mistarihi

Abstract—We have previously introduced an ultrasonic imaging approach that combines harmonic-sensitive pulse sequences with a post-beamforming quadratic kernel derived from a second-order Volterra filter (SOVF). This approach is designed to produce images with high sensitivity to nonlinear oscillations from microbubble ultrasound contrast agents (UCA) while maintaining high levels of noise rejection. In this paper, a two-step algorithm for computing the coefficients of the quadratic kernel leading to reduction of tissue component introduced by motion, maximizing the noise rejection and increases the specificity while optimizing the sensitivity to the UCA is presented. In the first step, quadratic kernels from individual singular modes of the PI data matrix are compared in terms of their ability of maximize the contrast to tissue ratio (CTR). In the second step, quadratic kernels resulting in the highest CTR values are convolved. The imaging results indicate that a signal processing approach to this clinical challenge is feasible.

Keywords— Volterra Filter, Pulse Inversion, Ultrasonic Imaging, Contrast Agent.

I. INTRODUCTION

INTERACTION between microbubbles UCAs and acoustic wave result in nonlinear harmonic echo generation. This phenomenon can be exploited to enhance the echoes from the microbubbles and, therefore, reject fundamental components resulting largely from tissue. Imaging techniques based on nonlinear oscillations have been designed for separating and enhancing nonlinear UCA echoes from a specified region of interest within the imaging field, including second harmonic (SH) B-mode imaging and pulse inversion (PI) Doppler imaging [4]. The SH imaging employs a fundamental frequency transmit pulse and produces images from the second harmonic component of received echoes by using a second harmonic bandpass filter (BPF) to remove the fundamental frequency. In order to increase UCA detection sensitivity in the limited transducer bandwidth condition, spectral overlap between fundamental and second harmonic parts need to be minimized by transmitting narrow-band pulses resulting in an inherent tradeoff between contrast and spatial resolution.

Mamoun F. Al-Mistarihi is with the Electrical Engineering Department, Faculty of Engineering, Jordan University of Science and Technology, P.O. Box 3030, Irbid 22110, Jordan. (phone: + (962) 2-7201000, fax: + (962) 2-7095018, email: mistarihi@just.edu.jo).

In PI imaging a sequence of two inverted acoustic pulses with appropriate delay is transmitted into tissue. Images are produced by summing the corresponding two backscattered signals. In the absence of tissue motion, the resulting sum can be shown to contain only even harmonics of the nonlinear echoes. The PI imaging overcomes the tradeoff between contrast and spatial resolution because it utilizes the entire bandwidth of the backscattered signals. As a result, superior spatial resolution can be achieved when compared with SH imaging. However, the subtraction process results in significant reduction of signal to noise as the harmonics are typically 20 - 30 dB or more below the (cancelled) fundamental component.

We have previously shown that the SOVF-based quadratic kernels provide high sensitivity to harmonic echoes comparable to PI with a significant increase in dynamic range due to inherent noise rejection of quadratic filtering [6]. An algorithm for deriving the coefficients of the kernel using singular values decomposition (SVD) of a linear and quadratic prediction data matrix was proposed and experimentally validated in [7]. Imaging results and comparisons with SH and PI images have shown that quadratic imaging is superior to SH and compares favorably with PI without the need for multiple transmissions. However, due to reliance on linear and quadratic prediction, the quadratic kernel has sensitivity to the fundamental that limits its ability to detect UCA in the microvasculature.

PI and quadratic imaging were combined in [8] to mitigate the limitations of both methods. The approach is based on quadratic filtering of PI data that, while noisy, is largely free of fundamental tissue components. The efficiency of the quadratic kernel in rejecting noise while maintaining quadratic signal components allows the recovery of quadratic components below the noise floor. This new quadratic PI (QPI) imaging approach offers the promise of detecting harmonic oscillations at or below the noise floor. Given the current trend of imaging UCA with extremely low transmit pulse amplitudes (to minimize nonlinear echo generation from tissue), the ability of QPI to detect quadratic signal activity below the noise floor becomes essential to the detection of harmonic activity in the 40 – 50 dB range below the fundamental.

In this paper, a two-step algorithm for computing the coefficients of the quadratic kernel leading to reduction of

tissue component and increase the specificity while optimizing the sensitivity to the UCA is presented. In the first step, quadratic kernels from individual singular modes of the data matrix are compared in terms of their ability of maximize the contrast to tissue ratio (CTR). In the second step, quadratic kernels resulting in the highest CTR values are convolved. In practice this is limited to two or three modes in order to avoid impractically large kernel size.

The approach is demonstrated experimentally using images from in vivo kidney after bolus injection with UCA. Illustrative Images of the kidney of a juvenile pig were obtained before and after infusion of contrast agent (SonoVue, Bracco, Geneva, Switzerland) at various concentrations. For example, at a concentration of 0.01 ml/kg, B-mode images (3 cycles at 1.56 MHz transmit frequency) show no quantifiable change due to the presence of the contrast agent. PI images without second harmonic (SH) filtering showed 10.2 dB enhancement and evidence of residual tissue components due to motion. On the other hand, quadratic images obtained using the standard SVD-based, QPI, and two step QPI (TS-QPI) algorithm produced CTR values of 23.1, 31.1 and 35.9 dB, respectively. Imaging results as well as the spectral contents of QPI data show a significant increase in harmonic sensitivity and reduction in noise levels. Similar results were obtained from imaging flow phantom under a variety of exposure conditions and UCA concentration levels. Implications of this approach on new forms of functional ultrasound imaging are discussed.

II. THEORY

A. Quadratic Pulse Inversion Ultrasonic Imaging (QPI)

The algorithm in this section is based on [6-8], which have shown the validity of a SOVF as a model for pulse-echo ultrasound data from tissue mimicking media. The response of a quadratically nonlinear system with memory $\hat{y}(n+1)$, can be predicted by a second order Volterra model of m past values as follows:

$$\hat{y}(n+1) = \sum_{i=0}^{m-1} y(n-i)h_L(i) \qquad (1)$$
$$+ \sum_{j=0}^{m-1}\sum_{k=j}^{m-1} y(n-j)y(n-k)h_Q(j,k)$$

Where $h_L(i)$ and $h_Q(j,k)$ are the linear and quadratic filter coefficients respectively. Using a segment of the RF data, a system of linear equations are formed and solved for elements of the quadratic kernel. Details of the algorithm to determine the quadratic kernel that provide maximum contrast enhancement have been described in [6-7].

In [8], we presented an algorithm of post beamforming second order Volterra filter on a pulse Inversion data (QPI) to combine the features of the two techniques, improve the contrast specificity, reduce the noise component in the tissue region and recover part of the tissue component which is completely cancelled in PI image.

Applying quadratic filtering to Pulse-inversion data (in that order) allows the cascade to efficiently mitigate the limitations of either imaging method applied alone. Specifically, PI processing efficiently removes fundamental tissue components, but amplifies the noise floor thus masking low-level harmonic activity. The quadratic kernel can be designed to efficiently remove noise throughout the spectrum while maintaining quadratic data, even below the noise floor, which is not possible with linear filters. On the other hand, the ability of PI processing to eliminate fundamental tissue components is essential because the quadratic kernel derived from a prediction model is often sensitive to correlated fundamental data.

B. Two-step procedure for optimization of contrast sensitivity and specificity

In this paper, instead of using just one singular mode, we present a two-step algorithm for computing the coefficients of the quadratic kernel. In the first step, quadratic kernels from individual singular modes of the data matrix are compared in terms of their ability of maximize the CTR. In the second step, quadratic kernels resulting in the highest CTR values are convolved. The new algorithm shows that it is more efficient than the previous ones in terms of the enhanced reconstructed image, reduction of tissue component and increasing the specificity while optimizing the sensitivity to the UCA. A two-dimensional (2D) autocorrelation is performed on h_{qconv}, i.e. the kernel after convolution, to alleviate ringing effects of the quadratic kernels, where h_{qconv} is the quadratic kernel resulting from the convolution of the highest sensitivity quadratic kernels, which give the highest CTRs. Furthermore, we apply the 2D autocorrelation on the resulting kernel to improve the spatial response of the filter. Therefore, the 2D autocorrelation of the quadratic kernel h_{qconv} is given by:

$$Q = \left(h_{qconv} \otimes h_{qconv}\right) \otimes \left(h_{qconv} \otimes h_{qconv}\right) \qquad (2)$$

where Q represents the quadratic kernel resulting after two applications of 2D autocorrelation on the quadratic kernel h_{qconv} and "$\otimes$" denotes the operation of 2D correlation. The quadratic image is produced by applying the quadratic filter coefficients of Q to the beamformed RF data throughout the PI image to estimate the quadratic component,

$$\hat{y}_Q(n+1) = \sum_{j=0}^{P-1}\sum_{k=j}^{P-1} y(n-j)y(n-k)Q(j,k) \qquad (3)$$

where P is the size of the Q matrix which depends on the number of singular modes used to compute h_{qconv}. A flowchart of this algorithm is shown in Figure 1. In practice this is limited to two or three modes in order to avoid impractically large kernel size.
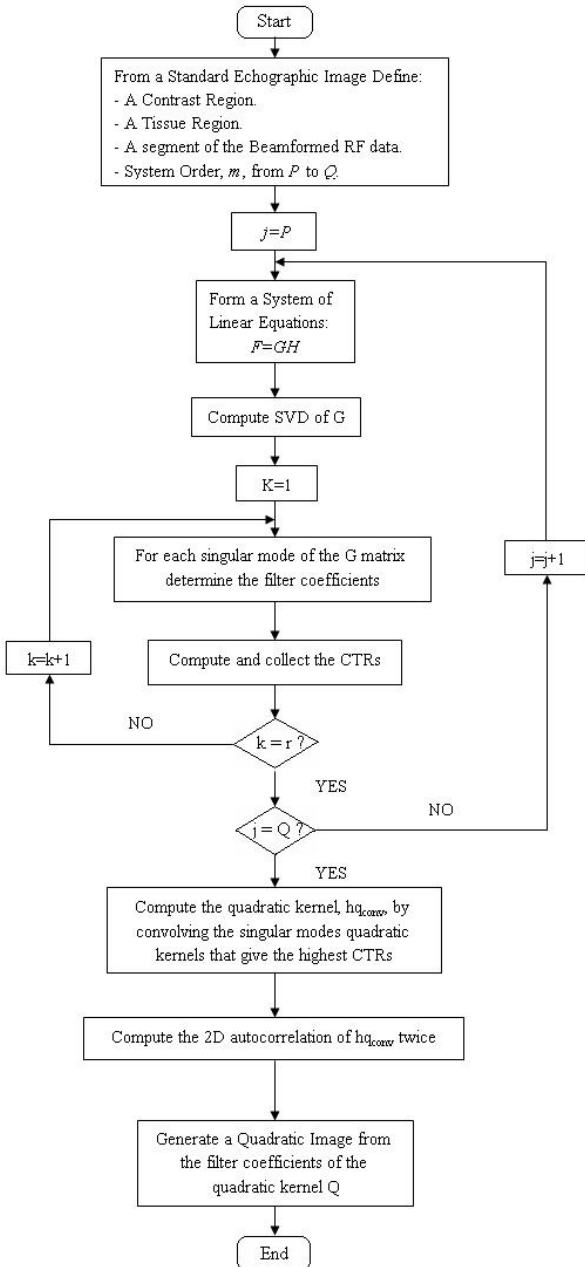
```
        ┌─────────┐
        │  Start  │
        └─────────┘
             │
┌──────────────────────────────────┐
│ From a Standard Echographic Image Define: │
│ - A Contrast Region.              │
│ - A Tissue Region.                │
│ - A segment of the Beamformed RF data. │
│ - System Order, m, from P to Q.   │
└──────────────────────────────────┘
             │
          ┌──────┐
          │ j=P  │
          └──────┘
             │
    ┌────────────────┐
    │ Form a System of │
    │ Linear Equations: │
    │     F=GH         │
    └────────────────┘
             │
    ┌────────────────┐
    │ Compute SVD of G │
    └────────────────┘
             │
          ┌──────┐
          │ K=1  │
          └──────┘
             │
    ┌───────────────────────────────┐
    │ For each singular mode of the G matrix │
    │ determine the filter coefficients │
    └───────────────────────────────┘
             │
    ┌───────────────────────────┐
    │ Compute and collect the CTRs │
    └───────────────────────────┘
             │
          ◇ k = r ?  NO → k=k+1
             │ YES
          ◇ j = Q ?  NO → j=j+1
             │ YES
```

Compute the quadratic kernel, hq_{conv}, by convolving the singular modes quadratic kernels that give the highest CTRs

Compute the 2D autocorrelation of hq_{conv} twice

Generate a Quadratic Image from the filter coefficients of the quadratic kernel Q

End

Fig. 1. A flowchart of the TS-QPI image generation algorithm.

III. MATERIALS AND METHODS

A. Experimental setup

We evaluated the algorithm with RF data acquired from experiments conducted *in vivo* on a juvenile pig. Bolus injections of SonoVue[TM] (Bracco Research SA, Geneva, Switzerland), an UCA consisting of sulphur hexafluoride gas bubbles coated by a flexible phospholipidic shell, were administered with two different concentrations (0.01 mL/kg

and 0.0025 mL/kg). Three- and four-cycle pulses at 1.56 MHz were transmitted using a convex array probe (CA430E) with amplitude 3.8 V to scan a kidney. Technos MPX ultrasound system (ESAOTE S.p.A, Genova, Italy) was modified so that a pair of inverted pulses with the appropriate time delay was subsequently transmitted to produce images with the PI technique. In addition, in order to remove low frequency components due to tissue motion artifacts and retain harmonic frequency components from UCAs, RF data from PI imaging were filtered using the linear highpass filter with cutoff frequency 2.3 MHz. For each setup, three frames of RF data from the PI technique were collected with 10 s and 15 s delays after the injection of 0.01 mL/kg and 0.0025 mL/kg UCAs, respectively. RF data were acquired with 16- bit resolution at 20-MHz sampling frequency without TGC compensation and saved for off-line processing.

B. Contrast measurements

As a comparison of contrast enhancement between images from different techniques, we determine CTRs from data in the RF domain before scan converted. CTRs of images can be calculated with echoes from two referenced regions: First, the contrast region inside the kidney (bottom-left part). Second, the tissue region outside the kidney (on the left hand side of the contrast region with the same depth). Both regions are composed of 21 connected A-lines with 7.5-mm axial extent.

IV. RESULTS AND DISCUSSION

Fig. 2 shows images obtained using a standard B-mode image of the kidney after the injection of 0.01 mL/kg UCAs acquired using 3-cycle transmission, PI, second harmonic on PI data (SHPI), quadratic image from twice 2D correlation of 38th singular mode of the B-mode data (QB), quadratic image from twice 2D correlation of the 2nd singular mode of the PI data (QPI), quadratic image from 2D correlation of the convolution of 1st and 2nd singular modes of the PI data (TS-QPI), separable, and truncated separable. Due to differences in dynamic ranges, each image is displayed with its full dynamic range as can be seen from the dB-level scale bars. Due to low microbubble populations in the perfused tissue of the kidney (Standard B-mode image), echogenicity from contrast regions is slightly lower than that from surrounding tissue regions, which agrees with the CTR value (-2.1175 dB) whereas the SHPI image provides CTR 14.3630 dB, echogenicity of the contrast region from the PI image appears brighter than that from surrounding tissue regions. Please note that the CTR value for the PI image without SH filtering was only 10.2319 dB, i.e. there is a 4.1311 dB gain due to the removal of tissue components introduced by motion. It is also worth noting that the SH image on the B-mode data suffers from significant loss in spatial resolution. The quadratic image from twice 2D correlation of 38th Singular mode provides CTR 23.1298 dB, which shows a contrast enhancement over the standard B-mode, PI, SHPI images.
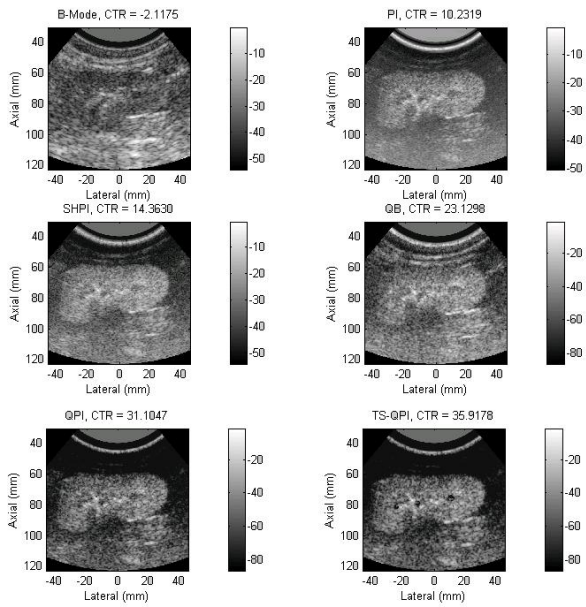
Fig. 2 Images of the: Standard B-mode image of the kidney at 10 s after the injection of 0.01 mL/kg, PI, SHPI, QB, QPI, and TS-QPI.

The quadratic image from twice 2D correlation of the 2nd singular mode of the PI data (QPI) is obtained using the algorithm described in section *II-A* with the use of a 5.6-mm contrast A-line and a system order 15, provides CTR 31.1047 dB, which shows a contrast enhancement over the previous four images.

The quadratic image from twice 2D correlation of the convolution of 1st & 2nd Singular modes of the PI data is obtained using the algorithm described in section 2.2 provides CTR 35.9178 dB, which shows a contrast enhancement over the standard B-mode, PI, SHPI QB, QPI images. We can clearly see not only the kidney's shape and boundary due to UCA echoes but also the large vascular structures. Also we can see that the kidney's shape and boundary due to UCA echoes are the clearest in the TS-QPI image compared with that in the standard B-mode, PI, SHPI QB, QPI images due to the fact that applying quadratic filtering to Pulse-inversion data (in that order) allows the cascade to efficiently mitigate the limitations of either imaging method applied alone. In addition, it can be seen that specular reflections of the TS-QPI image are the sharpest compared with that in the standard B-mode, PI, SHPI QB, QPI images.

Figure 3 shows the average spectra of data from the UCA and tissue region produced from the images shown in Figure 1 where the UCA spectra are shown in dark solid line (black) while the tissue spectra are shown in lighter solid line (red).
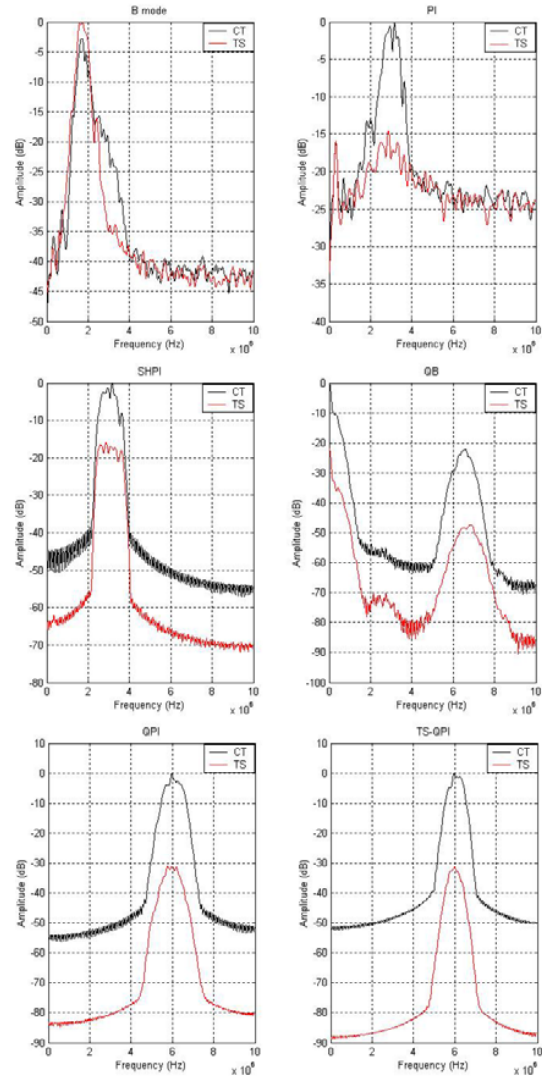

Fig. 3 Average spectra from the contrast (darker (black)) and tissue (lighter (red)) of the kidney: Standard B-mode, PI, SHPI, QB, QPI, and TS-QPI.

The spectra of the B-mode image shows spectral peaks at the fundamental and 2nd harmonic. It is interesting to see that the PI data and the SHPI data show spectral peaks at the 2nd harmonic due to the fact that the RF data from PI imaging were filtered using the linear highpass filter with cutoff frequency 2.3 MHz.
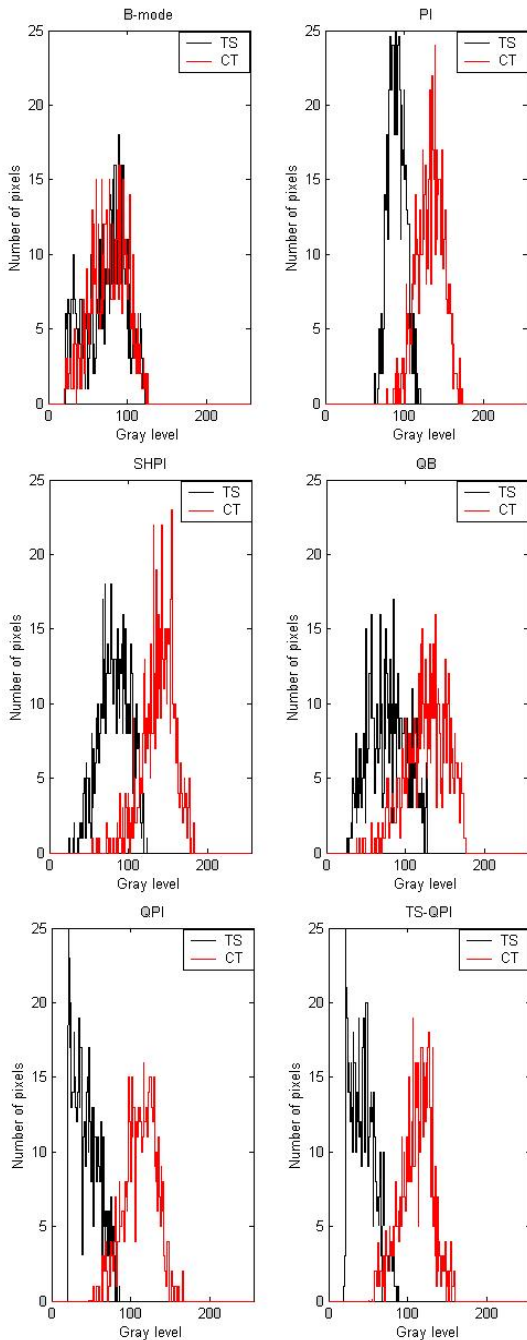
Fig. 4: Gray-level histograms produced from images shown in Figure 2. Histograms are produced from the contrast region (lighter (red)) and the tissue region (darker (black)).

The quadratic components show spectral peaks at low-frequency and at 6.6 MHz which is twice the 2nd harmonic of the B-mode image. In addition, spectra from the QPI, and TS-QPI images show a spectral peak at twice the 2nd harmonic of the B-mode image. Also from the spectra of the QPI, and TS-QPI images, the efficiency of the TS-QPI algorithm in rejecting noise while maintaining quadratic signal components allows the recovery of quadratic components below the noise floor.

Figure 4 shows the gray-level histograms produced from the Standard B-mode, PI, SHPI, QB, QPI, and TS-QPI images. In each case, the histogram from the UCA region is plotted with light solid line (red), while the histogram from tissue is plotted with darker solid line (black). One can see the degree of overlap between the histograms is highest for the standard B-mode image, whereas it is lowest for the quadratic from twice 2D correlation of the convolution of 1st & 2nd singular modes of the PI data (TS-QPI) image.

V. CONCLUSIONS

The results shown in this paper indicate clearly that TS-QPI imaging is far superior to either PI or quadratic imaging alone. This is due to the fact that applying quadratic filtering to Pulse-inversion data (in that order) allows the cascade to efficiently mitigate the limitations of either imaging method applied alone. Specifically, PI processing efficiently removes fundamental tissue components, but amplifies the noise floor thus masking low-level harmonic activity. The quadratic kernel can be designed to efficiently remove noise throughout the spectrum while maintaining quadratic data, even below the noise floor, which is not possible with linear filters. On the other hand, the ability of PI processing to eliminate fundamental tissue components is essential because the quadratic kernel derived from a prediction model is often sensitive to correlated fundamental data.

Also, the results shown in this paper clearly demonstrate the improved contrast sensitivity and specificity of the two-step algorithm presented in this paper. The first step of the approach identifies the modes with the highest level of sensitivity to contrast as measured by the CTR. This is an important step given the nature of SVD where the modes corresponding to the highest singular values may not be necessarily sensitive to nonlinear echoes from UCA. In the second step, the convolution of two or more contrast-enhancing quadratic kernels allows the 2D frequency passbands common to both kernels to be enhanced, while those non-overlapping passbands are reduced or eliminated. Given that the latter most likely result from "leakage" of linear and/or noise terms in the linear plus quadratic prediction, the convolution step offers a potentially powerful tool in improving the sensitivity and specificity to UCA by reducing these terms. Both CTR values and spectral contents of TS-QPI data compared to PI, SHPI, QB, and QPI data demonstrate the improved performance of this new approach.

REFERENCES

[1] K. I. Kim and E. J. Powers, " A digital method of modeling quadratically nonlinear systems with a general random input," *IEEE*

Trans. Acoust., Speech, Signal Processing, vol. 36, no. 11, pp. 1758-1769, Nov. 1988.

[2] T. Koh and E. J. Powers, " Second-order volterra filtering and its application to nonlinear system identification," *IEEE Trans. Acoust., Speech, Signal Processing,* vol. ASSP-33, no. 6, pp. 1445-1455, Dec. 1985.

[3] J. Ophir and K. J. Parker, " Contrast agent in diagnostic ultrasound," *Ultrasound in Med. & Biol.,* vol. 15, no. 4, pp. 319-333, Nov. 1989.

[4] D. H. Simpson, C. T. Chin, and P. N. Burns, " Pulse inversion Doppler: A new method for detecting nonlinear echoes from microbubble contrast agent," *IEEE Trans. Ultrason., Ferroelect., Freq. Contr.,* vol. 46, no. 2, pp. 372-382, March 1999.

[5] H. Yao, P. Phukpattaranont, and E. S. Ebbini, " Post-beamforming second-order Volterra filter for nonlinear pulse-echo imaging," in *Proc. ICASSP 2002,* 2002, pp. 1133-1136.

[6] P. Phukpattaranont and E. S. Ebbini, "Post-beamforming second-order Volterra filter for nonlinear pulse-echo ultrasonic imaging," *IEEE Trans. Ultrason., Ferroelect., Freg. Contr.*, vol. 50, no. 8, pp. 987-1001, Aug. 2003.

[7] P. Phukpattaranont, M. F. Al-Mistarihi and E. S. Ebbini, 'Post-beamforming Volterra filters for contrast-assisted ultrasonic imaging: In-vivo results," in *Proc. IEEE Ultrason. Symp*, 2003.

[8] M. F. Al-Mistarihi, E. S. Ebbini, "Quadratic Pulse Inversion Ultrasonic Imaging (QPI): Detection of Low-Level Harmonic Activity of Microbubble Contrast Agents," in *Proc.* ICASSP 2005, March 2005, vol. 2, pp. 1009-1012.

Mamoun F. Al-Mistarihi received the B.Sc. and M.Sc. degrees in Electrical Engineering from Jordan University of Science and Technology, Irbid, Jordan, M.E.E. and Ph.D. degrees in Electrical Engineering from University of Minnesota, Minneapolis, MN, USA, in 1992, 1996, 2005, and 2005, respectively. From 1994 to 2000, he was with the Royal Scientific Society, Amman, Jordan. Presently he is an Assistant Professor with the Electrical Engineering Department, Jordan University of Science and Technology, Irbid, Jordan. His research interests include signal processing, image processing, adaptive filtering, neural networks, and wireless sensor networks.